ACS OMEGA

Open Access

http://pubs.acs.org/journal/acsodf

Article

Characterization and Antibacterial Potential of Iron Oxide Nanoparticles in Eradicating Uropathogenic *E. coli*

Murad A. Mubaraki, Jaseem Ali, Baharullah Khattak,* Fozia Fozia, Taj Ali Khan, Mubbashir Hussain, Madeeha Aslam, Anisa Iftikhar, and Ijaz Ahmad*

Cite This: *ACS Omega* 2024, 9, 166−177

Read Online

ACCESS | Metrics & More | Article Recommendations

ABSTRACT: Proper management and control measurements are needed to stop the spread of highly pathogenic *E. coli* isolates that cause urinary tract infections (UTI) by developing new antibacterial agents to ensure the safety of public health. Therefore, the present investigations were used to achieve the synthesis of iron oxide nanoparticles (IONPs) via a simple coprecipitation method using ferric nitrates Fe $(NO_3)_3$ as the precursor and hydrazine solution as the precipitator and to explore the antibacterial activity against eradicating Uropathogenic *Escherichia coli* (*E. coli*). The synthesized IONPs were further studied using a UV−vis spectrophotometer, Fourier transform infrared spectroscopy (FT-IR), X-ray diffraction (XRD), and scanning electron microscopic (SEM) analysis. The maximum surface plasmon resonance peak was observed as absorption at 320 nm in a colloidal solution to validate the synthesis of IONPs. The FT-IR analysis was used to identify different photoactive functional groups that were responsible for the reduction of Fe $(NO_3)_3$ to IONPs. The crystalline nature of synthesized IONPs was revealed by XRD patterns with an average particle size ranging as 29 nm. The SEM image was employed to recognize the irregular morphology of synthesized nanoparticles. Moreover, significant antibacterial activity was observed at 1 mg/mL stock solution but after (125, 250, and 500 μg/mL) dilution, the synthesized IONPs showed moderate activity and became inactive at lower concentrations. The morphological and biochemical tests were used to confirm the presence of *E. coli* in the samples. Furthermore, the minimum inhibitory concentration (MIC) and minimum bacterial concentration (MBC) were carried out to determine the inhibitory concentrations for the isolated bacteria. The isolated *E. coli* were also subjected to antibiotic sensitivity testing that showed high resistance to antibiotics such as penicillin and amoxicillin. Thus, the findings of this study were to use IONPs against antibiotic resistance that has been developed in an inappropriate way.

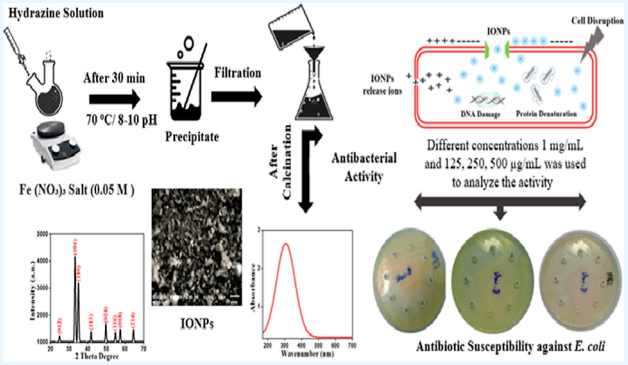

1. INTRODUCTION

In the 21st century, nanotechnology has flourished and become a major industrial field.[1] The particles with a size range between 1 and 100 nm in two or three dimensions were assist. The differences between the chemical and physical properties of nanoparticles are from their bulk microscopic forms.[2] In the 1980s, C60-Fullerene was recognized as an important nanoparticle.[3] Another important type of carbon-based nanoparticles was carbo-nanotubes regarded as crucial due to their significance in neurobiology applications.[4,5] In addition, many different types of nanoparticles including metal oxides or metal nanoparticles are available that consist of a metal oxide core surrounded by a ligand shell which shows a wide range of properties, both in solution and when isolated from the metal or bulk substance. Nanoparticles are considered for various applications, including as a catalyst,[6] in cosmetics,[7] and as an antibacterial agent[8] due to their extensive properties. The development of environmentally friendly products that were used in industrial processes has ignited a significant interest in using nanoparticles to address environmental issues such as contamination identification, removal, and prevention.[9] The Z-scheme iron oxide nanoparticles (IONPs) have heterostructure, derived from Fe−MOFs, which are applied to the photodegradation of tetracycline and methylene blue pollutants in wastewater.[10,11] The magnetic properties of IONPs are of great interest in different fields, including biotechnology and medicine,[8] where different chemical compounds serve as ligands for IONPs. It has been observed that the three-dimensional nanoparticle are longer than the

Received: May 4, 2023
Revised: July 21, 2023
Accepted: November 13, 2023
Published: December 26, 2023

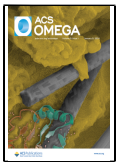

nanorods or nanowires, both of which have a size of less than 100 nm in the two dimensions.[12] When it comes to measuring the size and shape of nanoparticles, electron microscopy is one of the most reliable techniques. The morphology of nanoparticles is calculated using SEM, and the Scherrer equation is used to examine the particle size.[13] Dynamic light scanning (DLS) or photon correlation spectroscopy is used to calculate the hydrodynamic diameters of NPs in suspension.[14] Magnetite (Fe_3O_4), hematite (Fe_2O_3), maghemite (Fe_2O_3), and Wustite (Fe_2O_3) are the most common types of IONPs. Different methods like coprecipitation,[15] pulse laser decomposition,[16] electrochemical,[17] microemulsion,[18] surfactant-mediated/template synthesis,[19] forced hydrolysis,[20] and sol−gel[21] are used to synthesize IONPs. The coprecipitation procedures are highly efficient and straightforward chemical processes that can be used to synthesize IONPs in substantial amounts.[22]

IONPs have gained a great deal of interest in various fields such as food preservation,[23] ferrofluids, antibacterial activity,[24] biosensor,[25] magnetic refrigeration for MRI,[26] cell sorting,[27] targeted drug delivery,[28] and hyperthermic cancer treatments,[29] because of their specific properties. Recently, resistant bacterial strains have emerged, making it imperative to develop new antibacterial agents from a wide range of areas. Therefore, the need of attractive methods for the replacement antibacterial agents and lowering biofilm formation has emerged because of advancements in nanotechnology.[30] It is not well understood how nanoparticles are used to treat human cells, but their toxicity to bacteria has been well-documented for decades. The term UTI is used to describe a wide variety of medical conditions, from a life-threatening kidney infection to the presence of bacteria in the urine without any symptoms. Besides *Escherichia coli*, *Klebsiella* spp. *Pseudomonas*, *Staphylococcus saprophyticus*, *Enterococci*, and *Proteus mirabilis* have been linked to UTI.[31] Virulent *E. coli* strains cause urinary tract infections, food poisoning, and neonatal meningitis. Some of the cases have been reported for pneumonia, mastitis, septicemia, peritonitis, and hemolytic uremic syndrome.[32] Therefore, antibiotic resistance has been a critical issue in biomedical fields. So, the aim of the current investigation was to introduce new antibiotic resistance by using IONPs and testing them against Uropathogenic bacteria that cause UTI. There is no specific literature available on the eradicating Uropathogenic *E. coli* patients that cause UTI in district Kohat, KPK, Pakistan. Herein, in this article, we are reporting the synthesis of IONPs using the coprecipitation method and to explore their antibacterial activity in eradicating Uropathogenic *E. coli* for the first time. Further, the MIC and MBC were used to examine the inhibitory concentration of the isolated samples, and different biochemical tests were used to confirm the presence of *E. coli*. In this study, the effectiveness of commonly used antibiotics with that of IONPs was also used to determine the sensitivity of antibiotics against isolated bacteria. Accordingly, different antibiotics are available in local pharmacies without a prescription from a physician or doctor. The people with low literacy rates frequently overuse and misuse antibiotic. Therefore, it is essential to synthesize new antibacterial agents for antibiotic resistance. So, this work was carried out to synthesize IONPs using coprecipitation methods and then to explore the antibacterial applications of the synthesized IONPs.

2. MATERIAL AND METHODS

2.1. Synthesis of IONPs. The coprecipitation method was used to synthesize IONPs which is effective with a negligible effect on the environment. The solution was prepared in which water was mixed with a mixture of ferrous and ferric nitrates Fe $(NO_3)_3$ at a concentration of 0.05 M. After that, 50 mL of aqueous solution of (0.04 M) hydrazine was used as the precipitating agent that was mixed into the reaction mixture in a dropwise manner. The mixture was stirred at a ratio of 1:2 in a 250 mL conical flask using a magnetic stirrer for 30 min. Thereafter, the pH of the reaction rises after introduction of the hydrazine solution. The dark brown color change in the reaction mixture was observed. The UV−vis spectrophotometer was used to examine the reaction mixture. After 10 min of reaction, the maximum UV−vis peak was attained. Then, the aqueous solution was heated at 700 °C, using a hot plate stirrer, to obtain a precipitate of IONPs. The synthesized IONPs were collected after being drying in a furnace at 850 °C and were used for further characterization and biological evaluations.[33]

2.2. Characterization. The properties of IONPs were examined under different techniques that help to understand accurate, rapid, and reliable synthesis. The optical, structural, and morphological properties of synthesized IONPs were exposed to different characterization techniques including UV−vis, FT-IR, SEM, and XRD analysis. The UV−vis spectrum was obtained using a UV−vis spectrometer (U3900, Hitachi) at room temperature, and a quartz cuvette containing distilled water was used as a solvent at a scan rate of 300−800 nm/min. The crystallinity of the synthesized IONPs was measured using an X-ray diffractometer (Ultima IV model, Rigaku cooperation, Japan) operating with nickel-filtered Cu Kα (k51.54 Å), and the diffracted intensities were recorded from 20 to 70° at 2θ with a scan rate of 1 min^{-1} at 40 kV/40 mA current with dried IONPs on an XRD grid. While the FT-IR spectra were recorded using a spectrophotometer (Bruker Tensor-37 spectrometer, Germany) using KBr pellets in the 4000−400 cm^{-1} range at 4 cm^{-1} resolutions. The morphology of synthesized IONPs was done by SEM Version 1.0 (JSM-6510), at an accelerating voltage of 15 kV. In this analysis, the IONPs sample was shifted to a carbon grid, and the leftover sample was cleaned with blotting paper. Then, the newly created IONPs were captured after drying for 15 min under a mercury lamp. A high-pressure mercury lamp excited the retained molecule or proteins that showed autofluorescence.

2.3. Antibacterial Activity against Uropathogenic *Escherichia coli*. *2.3.1. Preparation of Stock Solution.* Stock solutions (1 mg/mL) of IONPs were prepared in dimethyl sulfoxide (DMSO) and subsequently diluted to 125, 250, and 500 μg/mL of concentrations, respectively.[34]

2.3.2. Collection of Bacterial Pathogens. Uropathogenic *E. coli* was sampled from patients at the Combine Military Hospital (CMH) in Kohat, KPK, Pakistan. These isolates were dispersed to the KUST Department of Microbiology in Kohat, Pakistan, and underwent standard testing protocols.[35]

2.3.3. Culture Media Preparation. In this analysis, 50 urine samples of *E. coli* were collected from patients in a CMH, Kohat. The Cystine-lactose-electrolyte-deficient agar (CLED) was used to inoculate the urine samples. The CLED media was used for the detection of urinary bacterial pathogens that help and develop the growth of microorganisms, specifically Gram-positive and Gram-negative bacteria. It was also used for the

https://doi.org/10.1021/acsomega.3c03078
ACS Omega 2024, 9, 166−177

isolation of urinary pathogens that provide different colonial morphology. After that, IONPs were subjected to standard microbiological identification procedures, including colony morphology, cellular morphology, and biochemical testing, to confirm their authenticity.[36] The Petri dishes, flasks, and test tubes were washed prior to being placed in a laminar flow hood, used to mix the CLED media, and then autoclaved for 15−20 min at 15 psi of pressure and 121 °C temperature. After being sterilized, the media flasks were transferred to the Laminar Flow hood to preserve them from contamination. In each Petri dish, 36 g of premix media was added and allowed to settle down. Aluminum foil was employed for covering the Petri plates to prevent contamination and then incubated at 37 °C for 24 h to check whether the medium was sterile under aerobic conditions. The samples were plated on CLED agar Petri plates in a biosafety cabinet and incubated for 24 h at 37 °C temperature. Incubation on CLED agar results in the detection of colonial growth. A method of subculturing was utilized to obtain genetically identical colonies. Standard biochemical tests were performed for identification of the isolated colonies of the pure culture including oxidase, catalase, Triple Sugar Iron (TSI) test, motility, indole, methyl red (MR), Vogues-Proskauer (VP), citrate utilization, and urease.

2.3.4. Purification by Different Media. The plates of MacConkey and Blood agar were further used to filter colonies. Colonies of nonlactose fermenters were a light brown color on MacConkey agar and a nonhemolytic white cream color on blood agar plates. The media was prepared by mixing 50 g of agar with 1 L of distilled water and subsequently heating the mixture until the agar was completely dissolved. The media was autoclaved at 121 °C and 15 ibs for 15 min, cooled to 50 °C, and then poured into sterile plates. The separation of Gram-negative bacteria was done by using MacConkey agar. It was used in the distinction of fermenting lactose from nonfermenting lactose Gram-negative bacteria. The isolation of pathogens from biological samples, water, and dairy products was accomplished. Additional bacterial cultures, such as UTI patients, were typically grown on a MacConkey agar medium.

2.4. Morphological Identification of *E. coli* Species. Gram staining was used to identify the *E. coli* species. The smear was made by placing a drop of normal saline on the slide of the microscope and mixing it into the bacterial colony. It was heated once the mixture was dried and treated with 0.5% crystal violet, which was then washed off with tap water after being left on for a minute. The slide was mordanted with 1% Lugol's iodine for 1 min and again washed with water for excess staining. The reaction was removed from the 95% alcohol after 30 s by washing it off with water, until color ceases to run out of the smear. It was dried at room temperature and observed under microscopic analysis. Pairs of Gram-negative reddish-pink rods were revealed.

2.5. Biochemical Identification of *E. coli*. Many other biochemical tests were used to positively identify *E. coli*, such as those for oxidase, catalase, TSI test, motility, indole, MR, VP, citrate utilization, and urease. Identification was made with the help of Bergey's Handbook of Systemic Bacteriology.[37]

2.5.1. Oxidase Test. The organism with a positive oxidase test has cytochrome oxidase. Enzymes like these are crucial for cellular respiration because they mediate the transport of electrons from the electron donor nicotinamide adenine dinucleotide hydrogen (NADH) to the electron acceptor ubiquinone (oxygen). An oxidizing agent created a compound with an indophenol blue color. The enzyme cytochrome oxidase can be identified by this biological method. The presence of cytochrome oxidase gives this product its distinctive purple color. On a tiny piece of filter paper, 1% oxidase reagent was dropped. A bacterial colony was mixed with the oxidase reagent on filter paper using a toothpick taken from a fresh bacterial culture plate left out overnight. Within 15−20 s, the color shift was observed. If the color changes to a deep purple in less than 10−20 s, the organism is classified as oxidase-positive. Negative results from the oxidase test were reported if the color did not change or if the reaction time exceeded 2 min.

2.5.2. Catalase Test. Microorganisms that may be tested for their production of the catalase enzyme can be categorized using this assay. With its ability to convert 3% hydrogen peroxide into harmless water and oxygen gas, this enzyme is a powerful tool in decontamination. For this experiment, we used a sterile toothpick to collect a bacterial colony that had been growing for 24 h and then cultured it on a microscope slide. The organism on the microscope slide was treated with one drop of 3% H_2O_2 from a dropper. Rapid bubble generation was seen after the Petri dish was covered to prevent the aerosol escape. If bubbles form, the catalase test was successful; otherwise, the result was likely negative.

2.5.3. Motility Test. Motility was examined by checking the flagella for movement. All of the organisms that are not able to move around on their own lack flagella. Differential medium brain heart infusion agar (BHI) with 0.5% agar was used for the semisolid Agar method of determining an organism's motility. Motile bacteria, when cultured on semisolid agar plates, grow in a swarming and dispersed pattern that can be seen by the naked eye. The unclear growth was widespread in the media. Contrary to the surrounding environment, growth is also observed along the stab line. On the contrary, when the bacteria are not motile, there is no evidence of diffusion, and the medium retains its transparency. There was a little tube of BHI agar, which is a semisolid medium for cultivating bacteria. The top of the test tube was used to avoid the release of any potentially harmful substances into the atmosphere. While collecting organisms from a single colony on plates cultivated for 18 to 24 h, a sterile inoculating loop or wooden toothpick was utilized. The medium was inoculated with a loop of a sterile inoculating loop (or a wooden toothpick). Bacterial growth was observed after incubating the test tube at 37 °C for 24 h following inoculation.

2.5.4. TSI Test. Differentiating bacteria in the gut is done with TSI media. Ingredients in the medium included phenol red, nutritional agar, 1% lactose, 0.02% ferrous sulfate, and 0.1% glucose. In this analysis, we used phenol red, a pH indicator. If the medium is acidic, the red phenol will change to a yellow color. The color of phenol red changes to violet when exposed to alkaline media. The medium will turn yellow if certain organisms absorb glucose in it. Because there is a finite amount of glucose in the medium, bacteria can oxidize amino acids to produce ammonia byproducts of their metabolism. The surface of the slope took on a purplish tint after ammonia was used to increase the pH. A crimson slant and a yellow dot indicate that glucose has been digested by the bacteria. Bacterial fermentation of sucrose and lactose resulted in a yellow solution. The formation of gas bubbles in the agar medium shows that the slant of the TSI successfully produces gas. H_2S reacts with ferrous sulfate to produce ferrous sulfide, a dark black precipitate. The inoculum from one culture was

https://doi.org/10.1021/acsomega.3c03078
ACS Omega 2024, 9, 166−177

placed on a fresh slant of TSI. The infected tube was incubated at 36 °C for 24 h, and the outcomes were evaluated.

2.5.5. Urease Test. With a urease test, we can identify the many types of bacteria that catalyze the conversion of urea into ammonia and carbon dioxide. Contaminating bacteria colonies were smeared onto urea agar plates by using a sterile loop. A change in color from yellow to pink on urea agar after overnight incubation is evidence that the organism produces urease.

2.5.6. Citrate Test. The ability to use citrate as a carbon and energy source is tested by subjecting isolated organisms to a citrate utilization test. A positive result indicates that citrate metabolism generates alkaline byproducts. The pH base's color-changing indicator shows that the medium has an acidic pH. Gram-negative bacteria and environmental isolates can be identified with the help of the citrate utilization test battery. To conduct the citrate test, a test tube containing potential pathogens was pierced with a straight sterile loop containing citrate agar. Overnight, the tubes were placed in an incubator for 30 h; a positive citrate test is indicated by a color change from blue to green in the citrate media, whereas a negative result shows no such change.

2.5.7. Indole Test. The ability of bacteria to catalyze tryptophan via the enzyme tryptophanase and generate indole is measured by this assay. There are three possible byproducts, and indole is one of them. Pyruvate and ammonium are the other two. To detect indole production, a reagent called Kovac's or Ehrlich's reagent is utilized. This reagent contains 4 (*p*)-dimethylaminobenzaldehyde, which reacts with indole to produce the red chemical quanidol. If the top of the test tube is circled in red, then the result is positive. The colony was transferred from the plates to the peptone water broth in the test tube using a sterile loop. When 2−3 drops of Kovac's or Ehrlich's reagent were added to the peptone water broth and allowed to incubate for 24 h, the results were visible.

2.5.8. Methyl Red Test. The goal of the experiment was to see whether the suspected microorganism under study could perform mixed acid fermentation in the presence of glucose. Lactic acid, succinic acid, and acetic acid are the three types of acids that result from this fermentation. The medium's pH is below 4.4 because of the high concentration of acid. Methyl red (*p*-dimethylaminoaeobenzene-*O*-carboxylic acid), a pH indicator, becomes yellow above pH 5.1 and red above pH 4.4, indicating that the pH level is quite low. Blue to red within a few minutes indicates a positive reaction. A wire loop was sterilized and then used to transfer a culture inoculum to a sterile tube of the Massachusetts Rental Voucher Program (MRVP) soup. After 37 °C incubation for 24 h, three-five drops of MR indicator solution were added to the tube.

2.5.9. Voges Proskauer Test. The VP test revealed that the bacterium produces acetoin via a butylene glycol metabolic pathway. Fermentation of glucose requires pyruvic acid. The test microorganisms were introduced into VP broth in screw-capped test tubes and then cultivated at 37 °C for 24−48 h. After a brief incubation period, 10 drops of Barrit reagent A (alpha-naphthol) and 5 drops of Barrit reagent B (40% KOH) were added. The acetoin byproduct is converted to diacetyl when exposed to potassium hydroxide (KOH). Creatine, a catalyst, is included in the reagent as well. The ensuing reaction gave off a reddish color. Assume the best when you see red. A single pure *E. coli* culture inoculum was transferred to a sterile tube of MRVP broth through a sterile wire loop. The infected tube was kept in a 36 °C incubator for 48 h. Three mL of Barrett reagent A and 1 mL of Barritt reagent B were added after 48 h. After 10−15 min of undisturbed shaking with oxygen in the medium-to-air pressure range, the outcomes were observed.

2.6. Preparation of Turbidity Standard (McFarland Standard). To keep a range of bacteria available for antibiotic susceptibility testing and identification, the turbidity of bacterial suspensions is checked using 0.5 McFarland equivalent standards as a quality control measure (Table 1).

Table 1. Chemicals Used in McFarland's Preparation

ingredients	concentration	quantity (mL)
sulfuric acid	0.18	99.5
barium chloride	0.048	0.5

Before use, the McFarland equivalence standard tube is inverted multiple times to ensure suspension homogeneity. By comparing the turbidity of the bacterial sample and McFarland Standard tubes against the black and white bars printed on the attached card, the turbidity was measured.

2.7. Bacterial Susceptibility Testing. *2.7.1. Agar Well Diffusion Method.* IONPs were tested for their antibacterial activity against pathogenic microbes using the same methods recommended by the National Council for Clinical Laboratory Standards (NCCLS, 2003). Bacterial cultures were diluted to a turbidity of 0.5 McFarland.

2.7.2. Antibacterial Activity. To study the isolated *E. coli*, we grew bacterial growth on Mueller Hinton Agar (MHA) media using sterile cotton swabs. Each Petri dish had a well drilled into it after the media had been set using a sterile cork borer. The antibacterial activity of 1 mg/mL nanoparticles was initially determined by cultivating bacterial growth on an MHA medium with cotton swabs. Then, a cork borer was used to drill four separate wells. Dimethyl sulfoxide (DMSO) was utilized as a negative control, and discs containing ciprofloxacin antibiotics were used as a positive control. The dilution of different concentrations of IONPs such as 125, 250, and 500 μg/mL was followed in DMSO that was tested for their ability to kill germs. Several concentrations of nanoparticles were present in each well. Next, we placed all of the MHA-medium-filled Petri dishes into a 35 °C oven for 30 h.[33] As the incubation period ended, the limiting volumes were calculated.

2.7.2.1. Minimum Inhibitory Concentrations. The concentration at which further bacterial growth is inhibited is known as the minimum inhibitory concentration (MIC). All samples underwent this procedure. MIC was performed using a range of dilutions. The dilution was made with the nourishing broth. To pinpoint the specific concentration at which the IONPs exert their effects, several dilutions were made, starting with a 1 mg/mL stock solution and proceeding down through 50, 100, and 200 μg/mL. After 24 h, the *E. coli* broth cultures were put through the McFarland test and transferred to autoclaved tubes. For 30 h at 36 °C, we incubated tubes with both negative and positive controls.[38] Tubes with MICs have an extremely low concentration, thereby suffocating any potential for expansion inside their confines.

2.7.2.2. Minimum Bactericidal Concentrations. Minimum bacterial concentration (MBC) is the minimum effective concentration for killing bacteria. The identical methods employed in MIC were also used in MBC. If there was no visible growth, the concentration would be referred to as MBC.

https://doi.org/10.1021/acsomega.3c03078
ACS Omega 2024, 9, 166−177

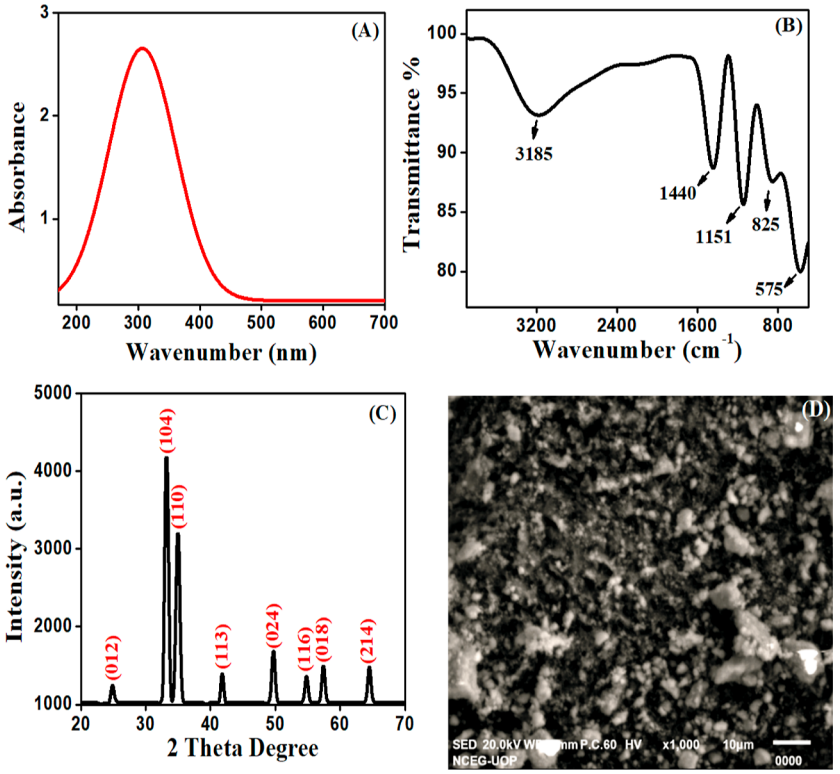

Figure 1. UV−vis spectroscopy of IONPs with 0.05 M concentrations of Fe $(NO_3)_3$ at 700 °C temperature for 30 min (A), FT-IR spectra of synthesized IONPs using KBr pellets in the 4000−400 cm^{-1} ranges at 4 cm^{-1} resolutions (B), XRD of IONPs from 20 to 70° at 2θ degree with a scan rate of 1 min^{-1} at 40 kV/40 mA (C), and SEM image of IONPs under 10 μm at an accelerating voltage of 15 kV (D).

The plates were kept in an incubator at 35 °C for 24 h. MBC is the concentration needed to prevent the spread of bacteria during the growth phase of a microorganism.

2.8. Ethical Statement. The ethical committee of Kohat University of Science & Technology, Kohat, Pakistan, approved the current work under Reference no. KUST/EC/00597 dated 14/10/2021.

3. RESULTS

The synthesis of IONPs was achieved by the coprecipitation method using ferrous and ferric nitrate as a precursor. The synthesis of IONPs was validated by UV−vis spectroscopic analysis by scanning the absorbance versus wavelength (λ), which is observed in Figure 1A. The characteristic peaks of IONPs were observed at 320 nm, which was due to charge transfer spectra. The electronic transition and optical band gap of the nanoparticles may be better comprehended through the use of UV−vis absorption analysis. As a result, the electronic transitions within the IONPs cause absorption near visible wavelength. Figure 1A shows the UV−vis absorption spectra of synthesized IONPs. The small bandgap energy of 3.87 eV was observed at a wavelength near 320 nm for synthesized IONPs samples.[39] Similarly, FT-IR analysis is an important technique used to investigate the different functional groups present in IONPs. In order to determine the functional groups and chemical bonding in the IONPs, the FT-IR analysis of the synthesized IONPs was examined in the regions of 400−4000 cm^{-1}. The FT-IR spectra of IONPs are shown in Figure 1B, as synthesized by the salt precursor $(Fe(NO_3)_3$ and hydrazine that act as a precipitating agent. The most characteristic functional group in FT-IR spectra was the O−H stretching vibration of the hydroxyl group of water molecules that can be observed in the broad absorption band at 3185 cm^{-1}.[40] Whereas, the strong and obvious absorption band that was obtained in the region of 825 and 575 cm^{-1} indicates the stretching vibration of Fe−O functional group of IONPs. The different bands in the FT-IR spectra of IONPs demonstrate that the presence of main functional groups, Fe−O and O−H, were observed in the respective region of the FT-IR spectra of IONPs after reduction indicated by the interaction among the iron salt precursor. The reduction and stabilization of IONPs are aided by this type of interaction.[41] Whereas, the average crystallite size and crystalline phases were accomplished using an X-ray diffraction pattern that was generated by using a wavelength of Cu−Kα radiation (λ = 0.15406 nm) over 2θ range of 20−70°, proceeding with a scanning rate of 2°/min. All the patterns exhibit the characteristic XRD pattern of hematite that was very similar to the (ICDD card no. 33-0664) standard diffraction pattern. All of the observed peaks were measured in accordance with the expected rhombohedral (hexagonal) structure of IONPs.[42] Figure 1C showed different diffraction peaks, confirming the crystalline nature of IONPs. The observed peaks correspond to the (012), (104), (110), (113), (024), (116), (018), and (214) at 2θ degrees of 24.6, 33.6, 35.0, 40.6, 49.6, 54.3, 57.3, and 64.4°. The high diffraction pattern resembles the formation of IONPs which has been confirmed by indicating the characterization peak occurring at 2θ = 33.6° with (104) plane which validates the crystalline nature of IONPs. The fwhm (full width at half-maximum) was used to calculate the mean particle size of the IONPs by using the Debye−Scherrer formula

$$D = K\lambda/(\beta\cos\theta) \quad (1)$$

https://doi.org/10.1021/acsomega.3c03078
ACS Omega 2024, 9, 166−177

where D represents the average particle size of nanoparticles, β identifies the value of the fwhm in the lines of X-ray diffraction, λ signifies X-ray radiation source wavelength of 0.15405 nm, θ is the half angle of diffraction (Bragg angle), and the Scherrer constant with a value from 0.9 to 1 is denoted by K. The above Debye−Scherrer equation was used to measure the average particle size of synthesized IONPs that was 29 nm.[43] Furthermore, SEM analysis was used to examine the surface morphology of the synthesized IONPs. Figure 1D shows the SEM images of the nanoparticles prepared by the coprecipitation method. In this figure, the synthesized nanoparticles showed the interaction between surface particulates that leads to the aggregate of the IONPs to some extent, whereas the particle size was measured in the range of 30−90 nm. The microscopic analysis show that high crystallinity emerged in the sample surface. Therefore, irregular morphology IONPs was obtained which was due to increase in the ratio of particle agglomeration that was noticed due to the electrostatic interaction between the layers of nanoparticles.[44] The chemical composition of the salt precursors such as nitrates or chlorides in a solvent (water) and in the presence of precipitating medium determines how the metal nanoparticle exits using coprecipitation methods. The present investigation can suggest a general mechanism for the synthesis of IONPs using the previously mentioned findings.[45] In this process, the reducing agent hydrazine reduces iron precursors into IONPs. Typically, the reaction is given by the following eq 2

$$Fe^{2+}+2Fe^{3+}+8OH\rightarrow Fe_3O_4+4H_2O \quad (2)$$

A number of iron precursors have been used to study the mechanisms of IONPs synthesis.[46] The concentration of the precursors, the reducing agents, and the addition rate of the reducing agents all have a significant effect on the reaction pathway for the synthesis of IONPs from precursor molecules through spontaneous nucleation and growth. The nature of the alkali may have an impact on the rate of the chemical reaction, the paramagnetic characteristics, and the degree of agglomeration of the synthesized IONPs. The ionic strength, temperature, and pH can also influence and change the particle sizes of nanoparticles. The development of different methods has also received a great deal of attention for the synthesis IONPs using chemical coprecipitation that yield stable, homogeneous, smaller-sized, and crystalline particles.[47]

3.1. Morphological and Biochemical Identification. The urine samples were collected from patients having urinary tract infections and were originally cultured on cysteine-, lactose-, and electrolyte-deficient (CLED) agar at the CMH in Kohat, KPK, Pakistan. In 20 out of 50 samples, *E. coli* was considered to be the source due to the presence of opaque yellow colonies with a darker yellow center. The samples were subcultures that showed pink to crimson colonies encircled by a bile salt precipitate on MacConkey Agar. The samples were then analyzed morphologically and biochemically to confirm the existence of *E. coli*. The Gram staining was used to determine that an organism was certainly *E. coli* based on its morphology. To confirm whether they contained *E. coli*, a biochemical test on urine samples was analyzed. The isolated bacteria were identified using the methods outlined in Bergey's manual of systemic bacteriology, including the use of oxidase, catalase, TSI, motility, indole, MR, VP, citrate utilization test, and urease. These biochemical tests were used to confirm the presence of *E. coli* in the samples. The results revealed that the isolates were found to be oxidase negative and catalase positive. The suspected Gram-negative bacteria were subjected to a series of biochemical tests that were particularly designed to detect *E. coli*. All of the isolates turned sugars, producing gas and acid through fermentation. According to Table 2, all isolates screened positive for the indole test were MR positive, citrate negative, urease negative, and VP negative. Furthermore, the positive mobility test was observed, and the TSI test showed positive for gas and negative for H_2S (Table 2).

Table 2. Standard Biochemical Tests Result for Uropathogenic *E. coli*, Collected From the Urine Sample of UTI Patients[a]

S. no	biochemical test	results
1	oxidase test	negative
2	catalase test	positive
3	motility test	positive
4	triple sugar iron	slant acid A butt acid A gas positive H_2S negative
5	citrate test	negative
6	indole test	positive
7	urease test	negative
8	methyl red	positive
9	Vogues Proskauer	negative

[a]The experiment was performed on CLED Agar in a biosafety cabinet and incubated for 24 h at 37 °C temperature.

3.2. Antibacterial Activity of IONPs by Agar Well Diffusion Method. Initially, 1 mg/mL IONPs was used to test the in vitro efficacy of antibacterial activity against *E. coli* cultures; DMSO was used as a negative control, and Ampicillin was used as a positive control. The antibacterial activity of the 1 mg/mL stock solution and the three more concentrations 125, 250, and 500 μg/mL were also analyzed. After performing concentration tests, an inhibition zone was determined. The more effective zone of inhibition was observed at a concentration of 1 mg/mL of IONPs against *E. coli*, in contrast to others, only four of 20 samples (at a 1 mg/mL concentration) showed moderate activity against *E. coli*. The samples (02, 09, 017, and 019) were completely inactive at 1 mg/mL concentration. Although samples (06 and 010) had the most active nanoparticles, the activity of samples (04, 05, 08, 011, 013, 014, 016, and 018) was also quite high. There was little to no difference in results between the samples when a 500 μg/mL concentration of IONPs was used, but there was a noticeable change in activity with 1 mg/mL concentration. The sample (019) was the least active of all of the samples tested, whereas several other samples tested at the highest levels of activity for iron oxide nanoparticles.

The activity was lowest in samples (02 and 019) at 250 μg/mL and second-lowest in samples (09 and 017). The most activity was found in sample (03), which ranked third out of 20 total samples. All samples had negligible activity at a concentration of 125 μg/mL of IONPs. There were certain samples (02, 09, 017, and 019) where the activity was not observed. Very low levels of activity were found in these samples with the highest levels found in the sample (014). Nanoparticle activity was observed in all but four samples (a surprising finding at this dosage). Both sample (06) and sample (010) were equally effective against all of the concentrations tested. Samples (04, 05, 08, 011, 013, 014,

https://doi.org/10.1021/acsomega.3c03078
ACS Omega 2024, 9, 166−177

Table 3. Antibacterial Activities of IONPs against Uropathogenic *E. coli* (1−20), Collected from the Urine Samples of UTI Patients[a]

samples	concentrations				positive control	negative control
	1 mg/mL (mm)	500 μg/mL (mm)	250 μg/mL (mm)	125 μg/mL (mm)	ciprofloxacin[c] (mm)	DMSO[b] (mm)
1	16 ± 2	13 ± 2	9 ± 2	7 ± 2	12 ± 2	0
2	13 ± 1	10 ± 2	6 ± 1	8 ± 1	5 ± 2	0
3	17 ± 1	16 ± 1	14 ± 1	9 ± 1	13 ± 1	0
4	18 ± 1	16 ± 1	12 ± 1	8 ± 1	14 ± 1	0
5	18 ± 1	14 ± 1	11 ± 1	8 ± 1	12 ± 1	0
6	19 ± 1	16 ± 1	13 ± 1	9 ± 2	12 ± 2	0
7	17 ± 2	15 ± 2	13 ± 1	9 ± 1	13 ± 1	0
8	18 ± 2	16 ± 1	12 ± 2	8 ± 1	12 ± 2	0
9	14 ± 2	9 ± 1	7 ± 1	6 ± 1	5 ± 1	0
10	19 ± 1	16 ± 1	13 ± 1	9 ± 1	14 ± 1	0
11	18 ± 1	16 ± 1	13 ± 1	9 ± 1	13 ± 2	0
12	17 ± 1	14 ± 1	11 ± 1	8 ± 1	12 ± 1	0
13	18 ± 2	16 ± 1	13 ± 1	9 ± 1	14 ± 1	0
14	18 ± 1	15 ± 1	13 ± 1	10 ± 1	12 ± 2	0
15	17 ± 1	15 ± 1	12 ± 1	9 ± 1	13 ± 2	0
16	18 ± 1	14 ± 1	12 ± 1	8 ± 1	12 ± 1	0
17	13 ± 2	10 ± 2	7 ± 2	6 ± 1	5 ± 2	0
18	18 ± 1	15 ± 2	12 ± 1	8 ± 1	13 ± 1	0
19	12 ± 1	8 ± 1	6 ± 1	9 ± 1	5 ± 1	0
20	17 ± 1	15 ± 1	13 ± 1	7 ± 1	12 ± 2	0

[a]The experiment was performed on MHA medium at 35 °C temperature in an oven for 30 h. [b]DMSO was used as a negative control. [c]Ciprofloxacin was used as a positive control.

Figure 2. Antibiotic susceptibility pattern against *E. coli* samples. The experiment was performed on MHA medium at 35 °C temperature in an oven for 30 h.

016, and 018) were present with activity in comparison to all other concentrations. The stock solution was diluted three times because of the potent antibacterial activity of iron oxide nanoparticles at a 1 mg/mL concentration. The usage of antibiotics served as the positive control, while DMSO served as the negative. In comparison to DMSO, antibiotics were quite active. Although antibiotics were effective as nanoparticles against all samples, their efficacy was reduced when applied to samples (02, 09, 017, and 019) (Table 3) See (Figure 2).

3.3. Antibiotic Susceptibility against *E. coli*. In this analysis, the antibiotic resistance of isolated Uropathogenic *E. coli* was examined. The goals of this study were to compare the performance of commonly used antibiotics with that of synthesized IONPs, to identify the antibiotic's sensitivity, and the resistance pattern against selected microorganisms. The antibiotics ciprofloxacin (CIP), levofloxacin (LEV), norfloxacin (NOR), imipenem (IPM), augmentin (AMC), tetracycline (TE), amoxicillin (AMC), penicillin (P), ceftazidime (CAZ), and ceftriaxone (CEF) were used to test the antibiotic susceptibility of Uropathogenic *E. coli*.

Table 4 lists the concentrations and acronyms of antibiotics employed in contemporary scientific research. These are the most widely used and accessible antibiotics. These antibiotics were used to determine the resistance pattern and intermediate

Table 4. Antibiotics are Used along with Their Potency for Antibiotic Susceptibility against Uropathogenic *E. coli*[a]

S. No	antibiotic	abbreviation	potency (μg)
1	norfloxacin	NOR	10
2	ciprofloxacin	CIP	5
3	imipenem	IPM	10
4	augmentin	AMC	30
5	ceftriaxone	CRO	30
6	tetracycline	TE	30
7	levofloxacin	LEV	5
8	amoxicillin	AMC	20
9	penicillin	P	10
10	ceftazidime	CAZ	30

[a]The experiment was performed on MHA medium at 35 °C temperature in an oven for 30 h.

https://doi.org/10.1021/acsomega.3c03078
ACS Omega 2024, 9, 166−177

Table 5. Table Pattern for Antibiotics Susceptibility against Uropathogenic *E. coli* Isolates[a]

S. No	antibiotics	abbreviation	potency (μg)	resistant		intermediate		sensitive	
				R (n = 20)		I (n = 20)		S (n = 20)	
				N	%	N	%	N	%
1	norfloxacin	NOR	10	4	20	4	20	12	60
2	ciprofloxacin	CIP	5	13	65	2	10	5	25
3	imipenem	IPM	10	11	55	5	25	4	20
4	augmentin	AMC	30	14	70	1	5	5	25
5	ceftriaxone	CRO	30	10	50	2	10	8	40
6	tetracycline	TE	30	14	70	2	10	4	20
7	levofloxacin	LEV	5	4	20	2	10	14	70
8	amoxicillin	AMC	20	20	100	0	0	0	0
9	penicillin	P	10	20	100	0	0	0	0
10	ceftazidime	CAZ	30	14	70	2	10	4	20

[a]The experiment was performed on MHA medium at 35 °C temperature in an oven for 30 h.

sensitivity against Uropathogenic *E. coli* isolates. These antibiotics are widely utilized in urban healthcare facilities.

In the current study, all the isolates were put through antibiotic susceptibility testing to assess whether these are resistant, intermediate, or sensitive to the antibiotics that were commonly administered to treat similar infections. 20% or more of the samples showed resistance against the antibiotics. The antibiotics with the lowest resistance rates were norfloxacin and levofloxacin, while the antibiotics penicillin and amoxicillin showed maximum resistance against *E. coli*. All the examined antibiotics showed that the samples (02, 09, 017, and 019) showed more resistance (Table 5) (Figure 2).
In this analysis, the MIC and MBC of IONPs were examined under different concentrations. The finding showed that the MIC describes the lowest concentration that was necessary to inhibit bacterial growth, in contrast to MBC analysis. The MBC and MIC for IONPs were examined using three different concentrations (200, 100, and 50 μg/mL) (Table 6).

These concentrations were used to examine the MBC and MIC analyses of IONPs toward Uropathogenic *E. coli*. The results revealed that not a single strain of *E. coli* destroyed IONPs at a concentration of 50 μg/mL which was the inhibitory concentration for all samples except 02, 09, 017, and 019. However, the MIC appeared to be 100 μg/mL for samples (02, 09, 017, and 019), while the MBC was observed to be 100 μg/mL for all other samples. MIC and MBC testing revealed that the antibacterial activity of samples (02, 09, 017, and 019) did not begin until a concentration of 250 μg/mL, which was different from their previous activities. The MBC for these four samples was 200 μg/mL, while the MIC was 100 μg/mL, indicating bactericidal action at that concentration (MIC).

4. DISCUSSION

IONPs have unique properties such as superparamagnetic behavior, biocompatibility, and chemical amendment of their surface morphology. Ascribed to its possessions, IONPs are expediently applied in the different biomedical applications including antimicrobial agents,[48] magnetic storage media, biosensing applications,[49] and targeted drug delivery.[50] The development of a simple and efficient process is required for the synthesis of IONPs. Therefore, the current study was used to synthesize IONPs by coprecipitation methods, which required multiple reaction steps that are required to obtain the final products. The coprecipitation method is particularly attractive because of its high purity, low cost, high homogeneity, short preparation time, relatively low reaction temperature, and well-crystallized product. The synthesis of IONPs was characterized using different techniques. The optical properties of the colloidal solution were examined under UV−Vis spectra, which showed an intense absorption peak due to surface plasmon excitation. The characteristic peak was obtained for the synthesized IONPs by using UV−Vis spectra at a wavelength of 320 nm. Similar findings have been reported earlier where the UV−visible absorbance spectra of synthesized IONPs were found at 298−301 nm.[51] X-ray diffraction analysis was used to determine the crystalline phases of IONPs. The results confirmed that the particle size was 29 nm, which was in close agreement with those of previously published data.[52] The morphology of IONPs was confirmed by SEM images, which showed that the particles are irregular in shape and agglomerated nanoparticles may be due to the magnetic characteristics of IONPs.[53] The agglomeration of IONPs also indicated a small surface-to-volume ratio of the particles. Moreover, the nonspherical shape formation can be explained by the shear produced during the stirring process.[54] Likewise, in accordance with these statements, the same results for SEM analysis were previously obtained.[55] Moreover, FT-IR spectroscopy was carried out to identify different functional groups present in IONPs. The result showed different peaks that indicated the formation of IONPs, According to Aliahmad and Nasiri Moghaddam et al., different peaks observed in FT-IR spectra showed the formation of IONPs that were responsible for the reducing agent.[56] Moreover, the coprecipitation approach is increasing, owing to an economically feasible way and an easy approach to scale up for nanoparticle production. Therefore, nanosized IONPs were used because of their surface chemistry, magnetic characteristics, and small size, all of which made them ideal for the investigation. Furthermore, the medical (neuro), biological fields, and engineering can all benefit from IONPs (e.g., magnetic storage medium or catalysis, their pigment function).[57,58] So, this investigation was carried out to determine the antibiotic resistance in patients of UTI caused by *E. coli*. One of the most common infections that require medical care and even hospitalization is UTI. Effective treatment and consideration are necessary that was based on the identification of the actual strain of UTI and drug with less resistance to that particular strain. The purpose of this research was to test the susceptibility of Uropathogenic *E. coli* isolated from patients

https://doi.org/10.1021/acsomega.3c03078
ACS Omega 2024, 9, 166−177

Table 6. MIC and MBC of Different Dilutions Used for IONPs toward Uropathogenic *E. coli*[a]

samples	activity	concentrations		
		200 μg/mL	100 μg/mL	50 μg/mL
1	MIC			≥
	MBC		≥	
2	MIC		≥	
	MBC	≥		
3	MIC			≥
	MBC		≥	
4	MIC			≥
	MBC		≥	
5	MIC			≥
	MBC		≥	
6	MIC			≥
	MBC		≥	
7	MIC			≥
	MBC		≥	
8	MIC			≥
	MBC		≥	
9	MIC		≥	
	MBC	≥		
10	MIC			≥
	MBC		≥	
11	MIC			≥
	MBC		≥	
12	MIC			≥
	MBC		≥	
13	MIC			≥
	MBC		≥	
14	MIC			≥
	MBC		≥	
15	MIC			≥
	MBC		≥	
16	MIC			≥
	MBC		≥	
17	MIC		≥	
	MBC	≥		
18	MIC			≥
	MBC		≥	
19	MIC		≥	
	MBC	≥		
20	MIC			≥
	MBC		≥	

[a]The experiment was performed on MHA medium at 35 °C temperature in an oven for 30 h.

to commonly used antibiotics and to assess the effectiveness of IONPs against these bacteria.[32] In the aftermath of antibacterial action, the concentration at which the antibacterial and bacteriostatic effects take place was found. The results showed the effectiveness of IONPs that inhibit or kill the Uropathogenic *E. coli* as well as the levels of antibiotic resistance that IONPs exhibit. Furthermore, different morphological and biochemical tests were carried out including oxidase, catalase, TSI, motility, indole, MR, VP, citrate utilization test, and urease for the confirmation of *E. coli* bacteria. The results showed that each isolate tested positive for the indole test and for MR and negative for citrate, urease, and VP. Additionally, a positive mobility test was noted, and a TSI test revealed positive results for gas but negative results for H_2S. This finding is highly correlated with the finding of Liu et al.[59] The antibacterial activity against the isolated samples was also examined by the synthesized IONPs for utilizing 1 mg/mL stock solution and analyzing the results.[34] Although some samples performed unexpectedly poorly against *E. coli* at a dosage of 1 mg/mL, the majority showed good activity. The mentioned samples (02, 09, 017, and 019) showed almost no activity at 1 mg/mL, whereas other samples observed exceptionally high levels of activity. IONPs showed maximum activity in samples (06 and 010). The IONPs were subsequently diluted to a concentration of 500 μg/mL and then 1 mg/mL. The data followed the same results as the higher concentrations. Nonetheless, some unexpected variation was found in the data. The IONPs activity was highest in many samples and lowest in the sample (09). The samples with the least activity at 250 μg/mL were (02 and 019), followed by (09 and 017). The most activity was found in sample (03), which ranked third out of 20 total samples. All samples had negligible activity at a concentration of 125 μg/mL of IONPs. There were certain samples (02, 09, 017, and 019) that did not show any activity, or very low levels of activity were found in these samples, and sample (014) showed maximum activity. IONPs were good on all of the tested samples, but four samples observed a surprising result at this dosage. So, the activity patterns were consistent across almost all samples except for those numbered (02, 09, 017, and 019). Similarly, Rawalpindi armed forces at the department of microbiology reported 63% of the incidence of *E. coli* related UTI.[60] A hospital-based study conducted in Lahore, Pakistan, reported that 83% of UTI patients were infected with *E. coli*. A study conducted in Peshawar, Pakistan, report that 77% of the UTIs that were presented to the hospital were due to *E. coli*. A study conducted in 2018 revealed that while investigating for uropathogenic infection, large number of female patients were infected with UTI compared with male.[61] Moreover, the antibiotic sensitivity test was performed on Uropathogenic *E. coli* with a wide range of drugs, including ciprofloxacin (CIP), levofloxacin (LEV), norfloxacin (NOR), imipenem (IPM), augmentin (AMC), tetracycline (TE), amoxicillin (AMC), penicillin (P), ceftazidime (CAZ), and ceftriaxone (CEF). Antibiotics with the lowest resistance rates were norfloxacin and levofloxacin. Penicillin and amoxicillin resistance was the greatest. Resistance to penicillin and amoxicillin was found at 100%, whereas resistance to norfloxacin and levofloxacin was only 20%. In the current study, all of the antibiotics were tested and samples (02, 09, 017, and 019) proved resistant. Similar conclusions were drawn from the literature about the effectiveness of ciprofloxacin against the uropathogenic bacteria that cause UTIs.[62] Additionally, a study found that *E. coli* UTI among patients was resistant to fluoroquinolone, coamoxiclav, and cotrimoxazole, and a less resistant and more prescribed antibiotic was Fosfomycin[63] despite the fact that a study similarly showed 58% ciprofloxacin resistance.[64] In contrast to the current investigation, ciprofloxacin showed 25% susceptibility with 65% antibiotic resistance against UTI caused by *E. coli*. After that, the stock solution was diluted to get concentrations used for MBC and MIC. The concentrations used were from 200, 100, and 50 μg/mL to dilute the stock solution. The MBC was determined to be 100 μg/mL that was due to its antibacterial activity against *E. coli*, while the minimum bacteriostatic concentration was determined to be 50 μg/mL due to its bacteriostatic effect on nearly all isolates except four isolates that were resistant to all antibiotics. In light of the ongoing investigation on antibiotic

https://doi.org/10.1021/acsomega.3c03078
ACS Omega 2024, 9, 166−177

resistance, the findings highlight the importance and utility of IONPs against UTI caused by *E. coli*. This antibiotic resistance has been developed because of the inappropriate use of antibiotics. Overuse and misuse of antibiotics contribute to antibiotic resistance; people with poor literacy levels are often ignorant of this problem. In the current era of increasing antibiotic resistance, it is essential to find and use innovative antibacterial drugs. IONPs are being studied as a potential nanoweapon against drug-resistant bacteria.

5. CONCLUSIONS AND RECOMMENDATIONS

The aim of the current investigation was to achieve the synthesis of IONPs using the coprecipitation method, owing to their high convenience, productivity, and affordability. The synthesized IONPs were successfully characterized by different techniques such as UV−vis, FT-IR, XRD, and SEM analysis. The small surface morphology of synthesized IONPs with size ranges as short as 30−90 nm was obtained from SEM images. Moreover, the synthesized IONPs were used to highlight the antibiotic resistance against eradicating Uropathogenic *E. coli*. The results revealed the effectiveness of IONPs against all of the bacterial samples. Hence, the synthesized IONPs exhibited maximum antibacterial activity against all of the tested samples at a concentration of 100 μg/mL. Furthermore, the MIC and MBC were used to analyze the inhibitory concentration of bacteria that showed maximum inhibition at 50 μg/mL concentrations for almost all of the samples. Moreover, we suggest that future studies should continue to corroborate the mechanism in which IONPs interact with that of Uropathogenic *E. coli* and demonstrate their potential by using electron microscopy such as TEM and SEM analyses.

■ ASSOCIATED CONTENT

Data Availability Statement

All the data generated and analyzed have already been incorporated into the study.

■ AUTHOR INFORMATION

Corresponding Authors

Baharullah Khattak − *Department of Microbiology, Kohat University of Science and Technology, Kohat 26000, Pakistan*; Email: dr.baharullah@kust.edu.pk

Ijaz Ahmad − *Department of Chemistry, Kohat University of Science & Technology, Kohat 26000, Pakistan*; orcid.org/0000-0002-9139-1611; Email: drijaz_chem@yahoo.com

Authors

Murad A. Mubaraki − *Clinical Laboratory Sciences Department, College of Applied Medical Sciences, King Saud University, Riyadh 11433, Saudi Arabia*

Jaseem Ali − *Department of Microbiology, Kohat University of Science and Technology, Kohat 26000, Pakistan*

Fozia Fozia − *Biochemistry Department, Khyber Medical University Institute of Dental Sciences, Kohat 26000, Pakistan*; orcid.org/0000-0002-4554-7427

Taj Ali Khan − *Department of Microbiology, Kohat University of Science and Technology, Kohat 26000, Pakistan; Institute of Pathology and Diagnostic Medicine, Khyber Medical University, Peshawar, Khyber Pakhtunkhwa 25100, Pakistan*

Mubbashir Hussain − *Department of Microbiology, Kohat University of Science and Technology, Kohat 26000, Pakistan*

Madeeha Aslam − *Department of Chemistry, Kohat University of Science & Technology, Kohat 26000, Pakistan*

Anisa Iftikhar − *Bio-science and Biotechnology, Clarkson University, Potsdam, New York 13699-5725, United States*

Complete contact information is available at: https://pubs.acs.org/10.1021/acsomega.3c03078

Author Contributions

Conceptualization: B.K., and I.A.; data curation: M.A.M, and J.A.; formal analysis: F.F, and M.H.; funding acquisition: M.A.M; investigation: M.A.M. and J.A; methodology: M.A.M., J.A., A.I., M.A., and F.F.; project administration: I.A and B.K.; resources: I.A.; supervision: B.K., and T.A.K; validation: I.A, T.A.K., and A.I; writing—original draft: M.A.M., J.A., and M.A; and writing—review and editing: B.K.; F.F., M.H.; and I.A. All authors have read and agreed to the published version of the manuscript.

Funding

The publication charges for this article are borne from the Researchers Supporting Project number (RSPD2023R655), King Saud University, Riyadh, Saudi Arabia.

Notes

The authors declare no competing financial interest.

■ ACKNOWLEDGMENTS

The publication charges for this article are borne from the Researchers Supporting Project number (RSPD2023R655), King Saud University, Riyadh, Saudi Arabia.

■ REFERENCES

(1) Mangematin, V.; Walsh, S. The future of nanotechnologies. *Technovation* **2012**, *32*, 157−160.

(2) Auffan, M.; Rose, J.; Bottero, J. Y.; Lowry, G. V.; Jolivet, J. P.; Wiesner, M. R. Towards a definition of inorganic nanoparticles from an environmental, health and safety perspective. *Nat. Nanotechnol.* **2009**, *4*, 634−641.

(3) Kroto, H. W.; Heath, J. R.; Brien, S. C.; Curl, R. F.; Smalley, R. E. C60: Buckminsterfullerene. *Nature* **1985**, *318*, 162−163.

(4) Iijima, S. Helical microtubules of graphitic carbon. *Nature* **1991**, *354*, 56−58.

(5) Malarkey, E. B.; Parpura, V. Carbon nanotubes in neuroscience. *Acta Neurochir. Suppl.* **2010**, *106*, 337−341.

(6) Jia, C. J.; Schuth, F. Colloidal metal nanoparticles as a component of designed catalyst. *Phys. Chem.* **2011**, *13*, 2457−2487.

(7) Kokura, S.; Handa, O.; Takagi, T.; Ishikawa, T.; Naito, Y.; Yoshikawa, T. Silver nanoparticles as a safe preservative for use in cosmetics. *Nanomedicine* **2010**, *6*, 570−574.

(8) Rai, M.; Yadav, A.; Gade, A. Silver nanoparticles as a new generation of antimicrobials. *Biotechnol. Adv.* **2009**, *27*, 76−83.

(9) Lee, H. Y.; Lee, S. H.; Xu, C. J.; Xie, J.; Lee, J. H.; Wu, B.; Leen Koh, A.; Wang, X.; Sinclair, R.; Wang, S. X.; et al. Synthesis and characterization of PVP coated large core iron oxide nanoparticles as an MRI contrast agent. *Nanotechnology* **2008**, *19*, 165101.

(10) Li, Y.; Xia, Y.; Liu, K.; Ye, K.; Wang, Q.; Zhang, S.; Huang, Y.; Liu, H. Constructing Fe-MOF-derived Z-scheme photocatalysts with enhanced charge transport: nanointerface and carbon sheath synergistic effect. *ACS Appl. Mater. Interfaces* **2020**, *12* (22), 25494−25502.

(11) Yang, J.; Zhou, J.; Huang, Y.; Tong, Y. Lanthanide-Based Dual Modulation in Hematite Nanospindles for Enhancing the Photocatalytic Performance. *ACS Appl. Nano Mater.* **2022**, *5* (6), 8557−8565.

(12) Cao, G.; Wang, Y. *Nanostructures and nanomaterials: synthesis, properties, and applications*; Imperial College Press: London, UK, 2004.

(13) Holzwarth, U.; Gibson, N. 'The Scherrer equation versus the 'Debye-Scherrer equation. *Nat. Nanotechnol.* **2011**, *6*, 534.

(14) Aberle, L. B.; Kleemeier, M.; Hennemann, O. D.; Burchard, W. Selection of Single Scattering from Multiple Scattering Systems by 3D Cross-Correlation. 2. Concentrated Polymer Solutions. *Macromolecules* **2002**, *35*, 1877−1886.
(15) Tian, Z. M.; Yuan, S. L.; He, J.; Li, P.; Zhang, S. Q.; Wang, C. H.; Wang, Y. Q.; Yin, S. Y.; Liu, L. Structure and magnetic properties in Mn doped SnO2 nanoparticles synthesized by chemical co-precipitation method. *J. Alloys Compd.* **2008**, *466* (1−2), 26−30.
(16) Thai, T. M. N.; Kim, S. R.; Kim, H. J. Synthesis Fe_2O_3 polymorph thin films via a pulsed laser deposition. *New Phys.: Sae Mulli* **2014**, *64*, 252−255.
(17) Starowicz, M.; Starowicz, P.; Żukrowski, J.; Przewoźnik, J.; Lemański, A.; Kapusta, C.; Banaś, J. Electrochemical synthesis of magnetic iron oxide nanoparticles with controlled size. *J. Nanopart. Res.* **2011**, *13*, 7167−7176.
(18) Darbandi, M.; Stromberg, F.; Landers, J.; Reckers, N.; Sanyal, B.; Keune, W.; Wende, H. Nanoscale size effect on surface spin canting in iron oxide nanoparticles synthesized by the microemulsion method. *J. Phys. D: Appl. Phys.* **2012**, *45* (19), 195001.
(19) Brahma, S.; Shivashankar, S. A. Surfactant-mediated synthesis of functional metal oxide nanostructures via microwave irradiation-assisted chemical synthesis. *MRS Online Proc. Libr.* **2009**, *1174*, 1174-V02.
(20) Sutens, B.; Swusten, T.; Zhong, K.; Jochum, J. K.; Van Bael, M. J.; Van der Eycken, E. V.; Brullot, W.; Bloemen, M.; Verbiest, T. Tunability of size and magnetic moment of iron oxide nanoparticles synthesized by forced hydrolysis. *Materials* **2016**, *9* (7), 554.
(21) Karami, A.; Monsef, R.; Shihan, M. R.; Qassem, L. Y.; Falah, M. W.; Salavati-Niasari, M. UV-light-induced photocatalytic response of Pechini sol-gel synthesized erbium vanadate nanostructures toward degradation of colored pollutants. *Environ. Technol. Innovat.* **2022**, *28*, 102947.
(22) Yao, K.; Peng, Z.; Fan, X. Preparation of nanoparticles with an environment-friendly approach. *J. Environ. Sci.* **2009**, *21* (6), 727−730.
(23) Berry, C. C.; Curtis, A. S. G. Functionalisation of Magnetic Nanoparticles for Applications in Biomedicine. *J. Phys. D: Appl. Phys.* **2003**, *36* (13), 198−206.
(24) Babes, L.; Denizot, B.; Tanguy, G.; Le Jeune, J. J.; Jallet, P. Synthesis of Iron Oxide Nanoparticles Used as MRI Contrast Agents: A Parametric Study. *J. Colloid Interface Sci.* **1999**, *212* (2), 474−482.
(25) Cf Chan, D.; B Kirpotin, D.; A Bunn, P. Synthesis and Evaluation of Colloidal Magnetic Iron Oxides for the Site-Specific Radio Frequency Induced Hyperthermia of Cancer. *J. Magn. Magn. Mater.* **1993**, *122* (1−3), 374−378.
(26) Beets-Tan, R. G. H.; Van Engelshoven, J. M. A.; Greve, J. W. M. Hepatic Adenoma and Focal Nodular Hyperplasia: MR Findings with Superparamagnetic Iron Oxideenhanced MRI. *Clin. Imag.* **1998**, *22* (3), 211−215.
(27) Matheson, L. J.; Tratnyek, P. G. Reductive Dehalogenation of Chlorinated Methanes by Iron Metal. *Environ. Sci. Technol.* **1994**, *28* (12), 2045−2053.
(28) Mahdy, S. A.; Rasheed, Q. J.; Kalaichelvan, P. T. Antimicrobial Activity of Zero-Valent Iron Nanoparticles. *Int. J. Mod. Eng. Res.* **2012**, *2* (1), 578−581.
(29) Mohapatra, M.; Anand, S. Synthesis and Application of Nano-Structured Iron Oxide/Hydroxides-A Review. *Int. J. Eng. Technol.* **2010**, *2* (8), 127−146.
(30) Ronald, A. The etiology of urinary tract infection: Traditional and Emerging Pathogens. *Am. J. Med.* **2002**, *113* (1), 14−19.
(31) Todar, K. Pathogenic E. coli. *Online Textbook of Bacteriology*; University of Wisconsin-Madison Department of Bacteriology, 2007.
(32) Kandpal, N. D.; et al. Co-precipitation method of synthesis and characterization of iron oxide nanoparticles. *J. Sci. Ind. Res.* **2014**, *73* (2), 87−90.
(33) White, P. A.; McIver, C. J.; Rawlinson, W. D. Integrons and gene cassettes in the Enterobacteriaceae. *Antimicrob. Agents Chemother.* **2001**, *45*, 2658−2661.
(34) Yao, K.; Peng, Z.; Fan, X. Preparation of nanoparticles with an environment-friendly approach. *J. Environ. Sci.* **2009**, *21* (6), 727−730.
(35) Gibreel, T. M.; Dodgson, A. R.; Cheesbrough, J.; Fox, A. J.; Bolton, F. J.; Upton, M. Population structure, virulence potential and antibiotic susceptibility of uropathogenic Escherichia coli from Northwest England. *J. Antimicrob. Chemother.* **2012**, *67* (2), 346−356.
(36) Owlia, P.; Nosrati, R.; Alaghehbandan, R.; Lari, A. R. Antimicrobial susceptibility differences among mucoid and non-mucoid Pseudomonas aeruginosa isolates. *GMS Hyg. Infect. Control* **2014**, *9* (2), Doc13.
(37) Liu, J. f.; Zhao, Z. s.; Jiang, G. b. Coating Fe_3O_4 magnetic nanoparticles with humic acid for highly efficient removal of heavy metals in water. *Environ. Sci. Technol.* **2008**, *42* (18), 6949−6954.
(38) Yang, C.; Yan, H. A green and facile approach for synthesis of magnetite nanoparticles with tunable sizes and morphologies. *Mater. Lett.* **2012**, *73*, 129−132.
(39) Srivastava, V.; Singh, P.; Weng, C.; Sharma, Y. Economically viable synthesis of Fe_3O_4 nanoparticles and their characterization. *Pol. J. Chem. Technol.* **2011**, *13* (2), 1−5.
(40) Nazari, M.; Ghasemi, N.; Maddah, H.; Motlagh, M. M. Synthesis and characterization of maghemite nano powders by chemical precipitation method. *J. Nanostruct. Chem.* **2014**, *4*, 99.
(41) Mandel, K.; Kolb, C.; Straber, M.; Dembski, S.; Sextl, G. Size controlled iron oxide nano octahedra obtained via sonochemistry and natural ageing. *Colloids Surf., A* **2014**, *457*, 27−32.
(42) Hua, J.; Gengsheng, J. Hydrothermal synthesis and characterization of monodisperse α-Fe_2O_3 nanoparticles. *Mater. Lett.* **2009**, *63* (30), 2725−2727.
(43) Arokiyaraj, S.; Saravanan, M.; Udaya Prakash, N.; Valan Arasu, M.; Vijayakumar, B.; Vincent, S. enhanced antibacterial activity of iron oxide magnetic nanoparticles treated with Argemone mexicana L. leaf extract: an in vitro study. *Mater. Res. Bull.* **2013**, *48* (9), 3323−3327.
(44) Arakha, M.; Pal, S.; Samantarrai, D.; Panigrahi, T. K.; Mallick, B. C.; Pramanik, K.; Mallick, B.; Jha, S. Antimicrobial activity of iron oxide nanoparticle upon modulation of nanoparticle-bacteria interface. *Sci. Rep.* **2015**, *5* (1), 14813.
(45) Samrot, A. V.; Sahithya, C. S.; Selvarani A, J.; Purayil, S. K.; Ponnaiah, P. A review on synthesis, characterization and potential biological applications of superparamagnetic iron oxide nanoparticles. *Curr. Res. Green Sustainable Chem.* **2021**, *4*, 100042.
(46) Khalil, M. I. Co-precipitation in aqueous solution synthesis of magnetite nanoparticles using iron (III) salts as precursors. *Arab. J. Chem.* **2015**, *8* (2), 279−284.
(47) Kandpal, N. D.; Sah, N.; Loshali, R.; Joshi, R.; Prasad, J. Co-precipitation method of synthesis and characterization of iron oxide nanoparticles. *J. Sci. Ind. Res.* **2014**, *73*, 87.
(48) Sharma, R.; Agrawal, V. V.; Srivastava, A. K.; Govind, G.; Nain, L.; Imran, M.; Kabi, S. R.; Sinha, R. K.; Malhotra, B. D. Phase control of nanostructured iron oxide for application to biosensor. *J. Mater. Chem. B* **2013**, *1* (4), 464−474.
(49) Vangijzegem, T.; Stanicki, D.; Laurent, S. Magnetic iron oxide nanoparticles for drug delivery: applications and characteristics. *Expet Opin. Drug Deliv.* **2019**, *16* (1), 69−78.
(50) Pattanayak, M.; Nayak, P. L. Green synthesis and characterization of zero valent iron nanoparticles from the leaf extract of Azadirachta indica (Neem). *World J. Nano Sci. Eng.* **2013**, *2* (1), 06−09.
(51) Farahmandjou, M.; Soflaee, F. Synthesis and characterization of α-Fe_2O_3 nanoparticles by simple co-precipitation method. *Phys. Chem. Res.* **2015**, *3* (3), 191−196.
(52) Chuan Lim, E. W.; Feng, R. Agglomeration of magnetic nanoparticles. *J. Chem. Phys.* **2012**, *136* (12), 124109.
(53) Gunes, D.; Scirocco, R.; Mewis, J.; Vermant, J. Flow-induced orientation of non-spherical particles: Effect of aspect ratio and medium rheology. *J. Non-Newtonian Fluid Mech.* **2008**, *155* (1−2), 39−50.
(54) Lassoued, A.; Dkhil, B.; Gadri, A.; Ammar, S. Control of the shape and size of iron oxide (α-Fe_2O_3) nanoparticles synthesized

https://doi.org/10.1021/acsomega.3c03078
ACS Omega 2024, 9, 166−177

through the chemical precipitation method. *Results Phys.* **2017**, *7*, 3007−3015.
(55) Monsef, R.; Ghiyasiyan-Arani, M.; Salavati-Niasari, M. Design of magnetically recyclable ternary Fe2O3/EuVO4/g-C3N4 nanocomposites for photocatalytic and electrochemical hydrogen storage. *ACS Appl. Energy Mater.* **2021**, *4* (1), 680−695.
(56) Aliahmad, M.; Nasiri Moghaddam, N. Synthesis of maghemite (γ-Fe_2O_3) nanoparticles by thermal-decomposition of magnetite (Fe_3O_4) nanoparticles. *Mater. Sci.* **2013**, *31*, 264−268.
(57) Yang, H. Nanoparticle-mediated brain-specific drug delivery, imaging, and diagnosis. *Pharm. Res.* **2010**, *27*, 1759−1771.
(58) Ansari, S. A.; Oves, M.; Satar, R.; Khan, A.; Ahmad, S. I.; Jafri, M. A.; Zaidi, S. K.; Alqahtani, M. H. Antibacterial activity of iron oxide nanoparticles synthesized by co-precipitation technology against Bacillus cereus and Klebsiella pneumoniae. *Pol. J. Chem. Technol.* **2017**, *19* (4), 110−115.
(59) Liu, H. Y.; Lin, H. C.; Lin, Y. C.; Yu, S. H.; Wu, W. H.; Lee, Y. J. Antimicrobial susceptibilities of urinary extended-spectrum beta-lactamase-producing Escherichia coli and Klebsiella pneumoniae to fosfomycin and nitrofurantoin in a teaching hospital in Taiwan. *J. Microbiol. Immunol. Infect.* **2011**, *44* (5), 364−368.
(60) Kibret, M.; Abera, B. Antimicrobial susceptibility patterns of E. coli from clinical sources in northeast Ethiopia. *Afr. Health Sci.* **2011**, *11*, 40−45.
(61) Scharff, A. Z.; Rousseau, M.; Mariano, L. L.; Canton, T.; Albert, M. L.; Fontes, M.; Duffy, D.; Ingersoll, M. A. Sex differences in IL-17 determine chronicity in male versus female urinary tract infection. *JCI Insight* **2019**, *4*, No. e122998.
(62) Kumar, S.; Dave, A.; Wolf, B.; Lerma, E. V. Urinary tract infections. *Disease-a-Month* **2015**, *61* (2), 45−59.
(63) Akbar, U.; Ali, M.; Ali, F.; Rashid, Y.; Ikramullah; Khan, K. N. Phenotypic Detection of Antibiotic Resistance and Production of Extended Spectrum Beta Lactamases in E. coli Isolated from UTI Patients At (HMC): Phenotypic detection of antibiotic resistance and beta-lactamases in e. coli isolated from UTI. *Pakistan Biomed. J.* **2022**, *5* (4), 103−108.
(64) Turpin, C. A.; Minkah, B.; Danso, K. A.; Frimpong, E. H. Asymptomatic bacteriuria in pregnant women attending antenatal clinic at komfo anokye teaching hospital, kumasi, ghana. *Ghana Med. J.* **2007**, *41* (1), 26.

https://doi.org/10.1021/acsomega.3c03078
ACS Omega 2024, 9, 166−177